THE ASTRONOMICAL JOURNAL VOLUME 111, NUMBER 1 JANUARY 1996

DISTRIBUTION AND CORRELATION OF AGE, ABUNDANCE, AND MOTION OF LOWER MAIN SEQUENCE STARS

OLIN J. EGGEN

Cerro Tololo Inter-American Observatory, National Optical Astronomy Observatories,[1] Casilla 603, La Serena, Chile
Electronic mail: oeggen@noao.edu

Received 1995 May 22; revised 1995 October 10

ABSTRACT

A sample of lower main sequence stars within 14 pc of the sun, with abundances determined from main sequence displacement and ages from surface fluxes of Ca II, yields (1) nine probable pre-main-sequence stars, (2) a preliminary evaluation of the change of zero point of the lower main sequence, in the $(M_I, R-I)$ plane, as a function of [Fe/H], (3) a relatively clear isolation of young and old disk stars in the (U,V) velocity plane, and (4) a rough correlation of [Fe/H] with age that shows a very slow decrease in both the mean abundance and the abundance range with increasing age. © *1996 American Astronomical Society.*

1. INTRODUCTION

The exclusive domains of old (OD, $t>2\times10^9$ yr) and young (YD, $t\leqslant2\times10^9$ yr) disk population objects in the (U,V) velocity plane has been discussed elsewhere (Eggen 1989a, 1995c). The division of populations at $\sim2\times10^9$ yr also divides the stars into those that burn helium in degenerate cores (OD) from those that do not (YD). The isolation, at the lowest velocities, of the young disk stars may be intuitively acceptable but the avoidance of the YD domain in the (U,V) plane by OD stars may not be. However, a demonstration of this exclusion is described in Sec. 4 using age indicators based on the flux of the Ca II H and K emission lines. These age indicators are roughly calibrated in Sec. 2 on the basis of stellar superclusters. Section 3 describes a sample of nearby stars and Sec. 4 contains an attempt to roughly approximate the relation between age and heavy element abundance for disk populations.

2. AGE AND SURFACE FLUXES IN Ca II

The known members of the Pleiades supercluster (Eggen 1995a) and the HR 1614 supercluster (Eggen 1992) that are also in the Gliese catalogue are listed in Table 1. The values of I and $R-I$ are on the system defined in Eggen (1982). The values of π (Clus) are those derived from supercluster membership and $\log F$ (Ca II) is from the compilation by Panagi & Mathioudakis (1993) where the fluxes are in ergs/cm^2/s. The correlations between $R-I$ and $\log F$ are shown in Fig. 1. The two superclusters are represented by

$$\log F\ (1.1\times10^8\ \text{yr}) = 6.63 - 1.28(R-I) \quad \text{Pleiades,} \quad (1)$$

$$\log F\ (4\times10^9\ \text{yr}) = 6.07 - 1.28(R-I) \quad \text{HR 1614.} \quad (2)$$

The ages of the superclusters (Eggen 1992, 1995b) are based on isochrones derived from stellar models. The difference between the observed and computed values of $\log F$ are 0.00 $\pm$0.23 dex from Eq. (1) and 0.00$\pm$0.09 dex from Eq. (2). These dispersions are undoubtedly caused by (a) the diverse origins of the values of $\log F$, which are based on diverse methods and (b) intrinsic variations in $\log F$. The low mass, young Pleiades dwarfs are known to be chromospherically active and to contain spotted, rotating stars that cause periodic light variations. The increased dispersion in $\Delta \log F$ for these objects, although based on only a few stars, probably reflects this chromospheric activity. The number of stars is unfortunately small but their distribution in Fig. 1 gives a strong sense of the reliability of the population division. It should be noted that the values of $\log F$(Ca II) , or $\log F$(Mg II), represent only one of the available measures of stellar age. The strength of Hα and x-ray activity are also useful in this context but are much less quantifiable. The Hα absorption, equivalent widths do appear to correlate closely with age (e.g., Eggen 1990; Stauffer & Hartman 1986) but for the youngest stars Hα emission dominates and is of less use in age dating. More recently x-ray fluxes for many stars have become available. All these activity indicators are undoubtedly interconnected and relate to stellar rotation (e.g., Simon 1992) but like the Hα emissions, the x-ray fluxes of individual stars vary over larger ranges than do the Ca II (or Mg II) fluxes which they present the most stable diagnostic for discriminating between stellar ages presently available.

The values of M_I [Eq. (3)] in Table 1 are from (Eggen 1993)

$$M_I = 4.56(R-I) + 3.95 \quad \text{Hyades.} \quad (3)$$

The Pleiades and HR 1614 supercluster members in Table 1,

[1]Cerro Tololo Inter-American Observatory, National Optical Observatories, operated by the Association of Universities for Research in Astronomy, Inc. (AURA), under cooperative agreement with the National Science Foundation.

 0004-6256/96/111(1)/466/10/$6.00

TABLE 1. Members of the Pleiades and Hr 1614 superclusters.

Gliese	Name	I	R-I	π Clus	π Trig	M_I Clus	M_I Comp	LogF CaII	Sp.T.	Note
Pleiades										
5	HR 8	$5^m.53$	$0^m.265$	0.078	0.067	+4.98	+5.15	6.40	K0 V	
117	HR 857	5.36	0.30	0.095	0.121	+5.31	+5.31	6.34	K2 V	
211	HD 37394	5.56	0.28	0.094	0.091	+5.43	+5.23	6.22	K1 V	X
212	+53.935	7.90	0.815			+7.77	+7.67	5.49	M2.5	X
490A	+36.2322	8.77	0.81	0.056	0.049	+7.51	+7.64	5.95	M0	X
490B	G 124-31	10.44	1.26			+9.18	--	5.14	M4	X
507.1	G 164-66	8.64	0.895	0.067	0.050	+7.83	+8.03	5.30	M2	
897	-17.6768	(8.91)	1.02	0.075	0.073	+8.30	+8.60	--	M5	X
898	Vys 864	7.33	0.53			+6.72	+6.37	5.63	K5 V	X
HR 1614										
176	+18.683	7.85	0.955	0.104	0.116	+7.93	+8.30	4.78	M2.5	
183	HR 1614	5.34	0.365	0.104	0.110	+5.42	+5.61	5.49	K3 V	
205	HD 36395	(6.80)	0.85	0.164	0.170	+7.91	+7.83	(4.92)	M1 V	X
365	HD 84035	7.06	0.43	0.068	0.068	+6.21	+5.91	5.48	K5 V	
522	HD 119217	8.31	0.555	0.042	--	+6.43	+6.48	5.44	M1	
673	HD 157881	6.07	0.595	0.115	0.112	+6.37	+6.65	5.29	K7 V	
747.3	HD 178445	8.04	0.565	0.050	0.050	+6.54	+6.52	5.22	K7 V	
839	G 215-20	8.92	0.70	0.042	0.041	+7.02	+7.14	5.37	M2	
862	HD 213042	6.72	0.36	0.068	0.076	+5.89	+5.59	5.78	K5 V	

Notes to TABLE 1.

205	**Equal component binary (Eggen 1992). The values in parenthesis are for the mean component.**
211/212	**98 arcsec separation.**
490AB	**17 arcsec separation.**
897	**Rapid orbital motion of equal components.**
898	**23 arcsec from 897. BF CVn.**

which have the same heavy element abundances as the Hyades (Eggen 1995b), both give a dispersion in M_I(Clus)$-M_I$ [Eq. (3)] of σ=0.22 mag. Leggett *et al.* (1994) question the linearity of Eq. (3) on the basis of stellar models but the available models for $R-I>+0.6$ mag ($T_e<4150$ K) are demonstrably in error (e.g., Eggen 1995b) and Eq. (3) holds to the end of the hydrogen burning main sequence (mass near 0.08 solar masses, Burrows *et al.* (1993)). The Hyades supercluster contains two very similar, equal component binaries near the main sequence limit,

Gliese		I, $R-I$ mean component		M_I Clus	M_I Eq. (3)	π Clus	π Trig	Mass ⊙
65AB	UV Cet	($9^m.83$)	1.70	$+11^m.72$	+11.70	$0^m.382$	$0^m.375$	0.09
472AB	FL Vir	(10.00)	1.58	+11.25	+11.15	0.195	0.215	0.09

The agreement between the luminosities derived from the cluster parallax and from Eq. (3) is excellent. The mass of the mean components are derived from the orbital elements of $P=26.52$ yr, $a=1.95$ arcsec for UV Cet (Geyer *et al.* 1988) and $P=16.2$ yr, $a=0.715$ arcsec for FL Vir (Heintz 1989).

Using observations of Mg II (2900A), Hufgnagel & Smith (1994) have also concluded that the members of the HR 1614 supercluster are uniformly of age$\geq 3\times10^9$ yr.

3. THE SAMPLE OF NEARBY STARS

Lower main sequence stars for which values of the Ca II flux are available (Panagi & Mathioudakis 1993), with (1) $R-I$ larger than 0.4 mag, to avoid evolutionary effects, and (2) trigonometric parallax larger than 0.070 arcsec, to minimize error in the luminosities, are listed in Table 2 which contains the number in the catalogue of nearby stars (Gliese 1969). The majority of proper motions are from the Carls-

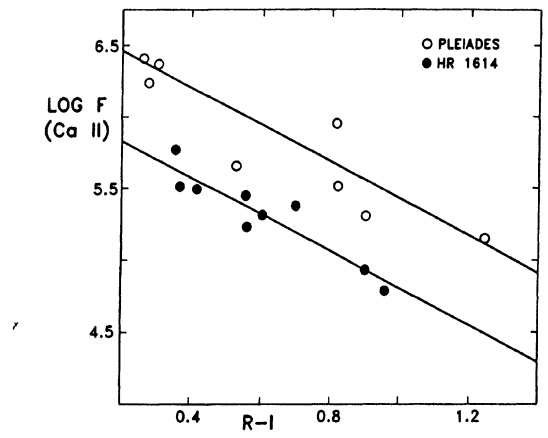

FIG. 1. The Pleiades and HR 1614 supercluster stars in the ($R-I$, log F) plane.

berg Meridian program (e.g., Carlsberg 1991) and reasonably accurate radial velocities are available for all of the stars.

The (M_V, $R-I$) relation is shown in Fig. 2 where the young disk stars, defined by their position in the U, V plane of Fig. 3, are designated by clear circles and the old disk by filled circles. The boundaries of the young disk domain in Fig. 3 are described in Eggen (1989a).

At least three reasons are available to explain deviations from the main sequence in Fig. 2. (1) The presence of undetected companions will place the stars above ([Fe/H]>0.1) or below ([Fe/H]<0.1) the Hyades main sequence. (2) The stars are still contracting to the main sequence. At the Hyades age the main sequence is linear over the range discussed here, as already noted, but at the Pleiades age ($\sim 10^8$ yr), for example, this linearity is broken near $R-I \sim 0.8-1.2$ mag (e.g., Prosser *et al.* 1991; Eggen 1995a) and redder stars are slightly elevated above the Hyades main sequence. The half-dozen objects, labeled in Fig. 2, all lie well above the main sequence and require separate attention:

Gleise	Trig	U	V km/s	W	ΔM_I
277A	0.″082	+6.2	−9.4	−16.8	+0.^m84
277B					+0.92
285	0.166	+12.9	−18.0	−10.3	+0.70
360	0.090	+33.6	−13.5	−13.9	+0.35
362					+0.51
380	0.118	+2.7	−10.0	+7.1	+0.54
669A	0.094	+35.3	−19.7	−4.2	+0.63
669B					+0.57
735	0.088	+9.7	−9.0	−6.8	+0.62,

where $\Delta M_V = M_V(\text{Obs}) - M_V$ [Eq. (3)]. These stars are almost certainly pre-main-sequence objects or undetected, near equal components binaries. The components of Gliese 277, 360/2, and 669 are undoubtedly pre-main-sequence stars. The components are equally displaced from the main sequence so undetected, equal components are an unlikely explanation for *both*. The same situation exists for Gliese 735, a known equal component spectroscopic binary (Duquennoy & Mayor 1988), with a period of 10.3d. Gliese 285 (YZ CMi) and 735 (V 1265 Aql) may show 1 min oscillations in the U-band photometry (Andrews & Staneck 1993). In the case of Gliese 735 the Ca II flux varies as much as 50% during these oscillations. Heintz (1993) has recently found an astrometric companion to Gliese 277A but this is too faint to appreciably affect the results in Table 2. He also confirms the trigonometric parallax. The consistency of the parallax determinations for Gliese 669AB is demonstrated by Harrington *et al.* (1985), who also list the individual values for Gliese 735: 0.089(M), 0.090(S), 0.097(V), and 0.078(USNO) arcsec and it is unlikely that parallax difficulties are responsible for the displacement of this star from the main sequence. The possibility, although probably remote, that the large displacements from the main sequence for these objects may result from large overabundances of heavy elements can only be tested with additional abundance determinations. It should be noted however, that the $J-H$ and $H-K$ indices, which may be sensitive to metallicity (e.g., Mould 1978), are indistinguishable from those of the Hyades and Pleiades clusters (e.g., Stauffer & Hartmann 1986).

The values of $\Delta M_I = M_I(\text{Obs}) - M_I$ [Eq. (3)] for the remaining stars listed in Table 2, with the exception of contributions from the small parallax uncertainties, probably are the result of a variation in heavy element abundance amongst the stars. At T_e=4500 K VandenBerg & Bell (1985) find that $R-I$ changes by only 0.01 mag over the range of [Fe/H] = +0.5 to −2.0 dex. Assuming that the $R-I$, T_e relation for the lower-temperature stars considered here is also essentially independent of [Fe/H], an empirical determination of the (ΔM_I, Δ[Fe/H]) relation can be obtained, as follows:

A. The Pleiades, Hyades, and HR 1614 supercluster members that define Eq. (3) have [Fe/H]=+0.1 dex (e.g., Eggen 1995a).

B. Some members of the 61 Cyg (Gliese 820AB) supercluster, which will be discussed elsewhere (but see Russell 1912; Eggen 1989b), in the relevant temperature range are as follows:

Gliese	I	$R-I$	π Clus	π Trig	M_I	ΔM_I
45	8.^m18	0.^m545	0.″048	0.″055	+4.^m60	−0.^m24
52	7.64	0.56	0.070	0.074	+6.87	−0.37
493	8.65	0.50	0.034	0.047	+6.81	−0.08
820A	4.12	0.46	0.295	0.295	+6.47	−0.42
820B	4.67	0.60			+7.02	−0.03
						−0.29

These stars are represented with plus signs in Fig. 4.

C. The following five stars are possible members of the Arcturus group (Eggen 1983);

TABLE 2. Nearby star sample.

Gliese	I	R-I	π Trig	μ_α/μ_δ 0".001	ρ km/sec	U	V km/sec	W	Sp.T.	LogF CaII	ΔLogF	M_I	ΔM_I	Note
1	6.55	0.93	0.225	5648/-2329	+23.4	+77.2	-99.5	-35.6	M4 V	4.23	+1.21	+8.31	-0.12	
2	8.03	0.85							M4 V	5.41	+0.13	+7.90	-0.07	X
4A	7.27	0.71	0.094	890/-207	+1.7	+36.8	-20.8	-18.2	K6 V	--	--	+7.14	+0.05	X
4B	7.33	0.71							K6 V	--	--	+7.20	-0.01	X
1002	10.16	1.63	0.215	-820/-1887	-42.0	-36.7	-41.2	+28.0	M	3.90	+0.64	+11.82	-0.44	
15A	6.09	0.87	0.282	2880/407	+11.3	+48.6	-12.2	-3.5	M1 V	4.55	+0.97	+8.34	-0.43	X
15B	8.36	1.24							M6 V	--		+10.61	-1.00	X
26	8.90	1.005	0.081	1545/46	-0.7	+60.4	-36.0	-0.9	M4	4.25	+1.09	+8.44	+0.09	
34B	6.07	0.59	0.170	1144/-537	+9.4	+36.3	-13.9	-19.4	M0 V	5.60	+0.27	+6.92	-0.28	X
47	8.70	0.985	0.088	356/-804	+10.2	+26.2	-3.5	-43.6	M3 V	5.03	+0.34	+8.43	+0.01	
49	7.56	0.89	0.110	725/99	-11.4	+22.0	-23.7	+5.6	M2 V	5.03	+0.46	+7.76	+0.24	
70	8.76	1.005	0.089	-477/-745	-25.5	-51.3	-21.6	-6.2	M2 V	3.72	+1.62	+8.38	+0.15	
79	7.34	0.68	0.082	852/0	+13.4	+39.7	31.9	-1.3	M1	5.23	+0.53	+6.91	+0.14	
82	(10.23)	1.285	0.082	300/-330	-9.8	+6.4	-18.5	+3.6	M4	5.44	-0.45	+9.80	0.00	X
96	7.53	0.775	0.095	215/43	-37.2	-19.9	-30.4	+14.4	M1.5	5.05	+0.59	+7.42	+0.06	
105A	4.96	0.37	0.139	1807/1457	+26.0	+76.6	-1.1	+31.9	K3 V	5.85	+0.31	+5.67	-0.03	X
105B	8.97	1.255							M	--	--	+9.68	-0.01	X
109	8.34	1.075	0.133	860/-341	+30.9	+40.5	-15.9	-12.8	M4	4.67	+0.58	+8.85	0.00	X
156	7.448	0.62	0.072	5/552	+63.8	+66.6	+12.2	-28.3	M0	4.73	+1.11	+6.77	+0.01	
166A	3.72	0.31	0.205	2226/-3420	-42.7	-100.0	-13.4	-45.3	K1 V	5.81	+0.42	+5.28	+0.08	X
166B	8.27	1.31							M2 V	4.80	+0.15	+9.83	+0.09	X
167	6.59	0.43	0.075	286/391	-23.2	+37.1	-8.1	+46.5	K5 V	5.55	+0.53	+5.97	-0.06	
169	6.86	0.62	0.100	-73/178	-33.0	-32.0	+6.0	+13.0	M1					
174	7.00	0.49	0.075	-238/-253	+7.4	+2.8	-2.4	-16.1	K3 V	6.18	-0.18	+6.38	-0.20	
192	8.69	0.95	0.075	283/238	-29.6	-24.2	+3.7	+28.6	M3 V	4.51	+0.90	+8.07	+0.21	
195A	8.30	0.90	0.080	79/-423	+30.2	+36.4	-12.7	-8.4	M2	5.38	+0.10	+7.87	+0.18	X
226	8.31	1.01	0.106	55/-1308	-21.0	+33.9	-47.4	-21.5	M3	4.86	+0.48	+8.45	-0.11	
239	7.94	0.735	0.099	-76/340	-57.1	-44.6	+44.6	-29.3	M1 V	5.25	+0.44	+7.92	-0.62	
250A	5.70	0.38	0.106	-550/-4	-9.3	-1.4	+15.0	-21.5	K5 V	5.58	+0.56	+5.83	-0.17	
250B	7.96	0.95							M2	4.72	+0.69	+8.09	+0.19	
251	4.61	1.115	0.175	-57/-426	+23.0	+27.6	-4.3	-14.9	M4	4.79	+0.41	+8.83	+0.20	
273	7.25	1.215	0.268	588/-3679	+18.5	-8.1	-51.8	-12.0	M3.5 V	4.75	+0.29	+9.39	+0.10	
277A	8.30	1.065	0.082	-247/-246	-0.7	+6.2	-9.4	-16.8	M3	5.21	+0.05	+7.87	+0.94	X
277B	9.17	1.23							M4	5.35	-0.30	+8.74	+0.82	X
278(C)	(9.05)	0.78	0.083	-171/-100	+2.5	+6.2	-3.0	-9.3	M0.5 V	5.68	-0.05	+7.65	-0.14	X
285	8.31	1.35	0.166	-352/-456	+18.6	+12.9	-18.0	-10.3	M4 V	5.32	-0.42	+9.41	+0.70	X
310	7.64	0.71	0.078	-1060/45	+11.0	+44.5	+14.4	-45.7	M1	5.47	+0.25	+7.10	+0.09	
330	8.59	0.85	0.070	-14/-329	-13.1	-16.3	-13.1	-15.9	M2	4.70	+0.84	+7.82	0.00	
338A	6.02	0.68	0.166	-1553/-631	+11.3	+41.1	-15.6	-21.7	M0 V	5.65	+0.11	+7.12	-0.07	X
338B	6.10	0.69							M0 V	5.62	+0.13	+7.20	-0.10	X
360	8.39	1.00	0.090	-366/-310	+5.4	+33.6	-13.5	-13.9	M3	4.99	+0.36	+8.16	+0.35	X
362	8.82	1.13							M4	--	--	+8.59	+0.51	X
373	7.25	0.73	0.098	-274/-556	+12.5	+22.8	-23.0	+10.0	M1	5.55	+0.15	+7.21	+0.07	
380	5.08	0.62	0.222	-1353/508	-26.2	+6.9	-19.1	-35.0	K8 V	5.40	+0.44	+6.81	-0.04	
382	7.23	0.92	0.118	-110/-246	+9.1	+2.7	-10.0	+2.1	M2	5.08	+0.37	+7.60	+0.54	
393	7.54	0.965	0.130	-518/-713	+9.0	+7.7	-30.6	-15.9	M2	4.23	+1.16	+8.11	+0.24	
408	7.78	1.035	0.145	-397/-290	+2.0	+8.0	-12.6	-4.4	M3	4.44	+0.87	+8.59	+0.08	
410	7.81	0.775	0.090	157/-45	-14.2	-12.8	+4.2	-9.8	M2	5.19	+0.45	+7.58	-0.10	
411	5.44	0.915	0.397	-569/-4031	-84.8	-46.1	-52.8	-7.44	M2 V	4.23	+1.23	+8.43	-0.31	
412A	6.81	0.82	0.184	-4380/870	-68.7	+133.7	-5.8	-10.4	M2 V	4.90	+0.68	+8.18	-0.50	X
436	8.43	1.03	0.106	900/-810	-9.5	-48.3	-17.9	+19.0	M3	4.67	+0.64	+8.56	+0.08	
445	8.29	1.20	0.196	715/482	-113.2	-67.5	-56.6	-79.2	M4	4.18	+0.91	+9.75	-0.33	
450	7.80	0.875	0.112	-265/273	0.0	+14.5	+5.1	-4.0	M1 V	4.91	+0.60	+8.05	-0.11	
453	6.00	0.42	0.102	-1077/-619	+49.0	+19.0	-73.0	-6.3	K5 V	5.74	+0.35	6.04	-0.18	
488	6.92	0.66	0.100	-38/-390	+4.8	-8.5	-16.5	-4.6	M0.5 V	5.58	+0.20	+6.92	+0.04	
494	7.79	0.865	0.095	-637/-16	-12.3	+27.5	-15.4	-11.5	M2	5.92	-0.40	+7.68	+0.21	
514	7.18	0.815	0.138	1125/-1078	+13.3	-54.4	-7.9	-3.9	M1 V	5.19	+0.40	+7.98	-0.31	
525	8.08	0.67	0.078	439/-1046	+22.6	-92.4	-72.3	-8.5	M0 V	5.12	+0.65	+7.60	-0.60	
526	6.58	0.855	0.195	1774/-1444	+75.2	-57.6	-1.5	-1.7	M3 V	5.06	+0.48	+8.03	-0.18	
551	7.16	1.635	0.761	-3406/715	-22.0	+29.0	+1.0	+14.0	M5 V	4.80	-0.26	+11.57	-0.17	X
570A	4.77	0.40	0.172	1009/-1663	+30.0	-42.3	-19.7	-16.9	K5 V	5.20	+0.91	+5.95	-0.18	X
570B	(6.87)	(0.885)							M2 V	(4.78)	(+0.72)	(+8.05)	(-0.06)	X
588	7.07	1.04	0.169	-1195/-1020	+9.2	+11.2	-41.3	-1.5	M4	4.50	+0.80	+8.21	+0.48	
617A	7.00	0.68	0.100	-494/89	-22.0	+8.7	-30.6	+1.4	M0 V	5.59	+0.17	+7.00	+0.05	X
617B	8.38	1.085							M3	--	--	+8.38	(+0.52)	X
649	7.81	0.835	0.102	-116/-487	+2.5	-18.8	-14.0	+0.4	M2	5.36	+0.30	+7.85	-0.09	
653	6.59	0.49	0.094	-922/-1144	+34.0	-46.7	-63.0	+21.3	K5 V	5.22	+0.78	+6.46	-0.28	X
654	8.08	0.91							M3 V	--	--	+7.95	+0.15	X
669A	8.90	1.195	0.094	-221/360	-34.8	+35.3	-19.7	-4.2	M4	5.29	-0.19	+8.77	+0.63	X
669B	9.94	1.41							M5	--	--	+9.81	+0.57	X
674	7.07	1.03	0.216	566/-872	-20:	+23.5	+2.0	-19.0	M4	4.76	+0.55	+8.74	-0.09	
686	7.75	0.87	0.126	931/1018	-12.2	+35.6	+33.5	-21.2	M1	5.07	+0.45	+8.25	-0.33	
699	6.83	1.26	0.555	-750/10315	-110.0	+91.4	-57.6	-21.6	M5 V	4.24	+0.77	+10.55	-0.85	
701	7.58	0.865	0.128	560/-330	+31.7	-32.2	+13.9	-19.8	M2 V	4.81	+0.71	+8.12	-0.23	
707	7.10	0.53	0.073	134/-417	-2.0	+9.4	-18.7	-19.3	K7 V	5.56	+0.39	+6.42	-0.05	
720A	8.12	0.74	0.074	456/369	-28.0	+35.0	-9.1	-30.2	M2	5.44	+0.24	+9.77	-0.26	X
720B	10.42	1.22							M	--	--	+8.90	-0.07	X
725A	6.58	1.07	0.290	-1342/1826	+24.2	-13.1	+24.9		M4	3.88	+1.38	+8.90	-0.07	X
725B	7.24	1.135							M4	3.63	+1.52	+9.56	-0.44	X
726	7.48	0.545	0.070	-133/-275	+17.7	-25.6	-9.9	-0.5	M0	5.39	+0.54	+6.68	-0.24	X

	I	$R-I$	π Clus	π Trig	M_I	ΔM_I
Gliese 181.1	10^m.38	0^m.75	0".041	0".056	+8^m.45	−1^m.08
G48−25	10.34	0.725	0.042	0.022	+8.50	−1.24
G10−25	8.96	0.525	0.053	0.034	+7.57	−1.23
L46−96	11.01	1.265	0.095	···	+10.90	−1.19
Gliese 821	8.96	0.855	0.092	0.087:	+8.80	−1.09
						−1.16

TABLE 2. (continued)

Gliese	I	R-I	π Trig	μ_α/μ_δ 0".001	ρ km/sec	U	V km/sec	W	Sp.T.	LogF CaII	ΔLogF	M_I	ΔM_I	Note
729	7.76	1.30	0.345	690/-207	-10.0	+11.0	-0.7	-7.9	M4.5	4.95	+0.02	+10.46	-0.58	X
731	8.42	0.74	0.074	-242/-480	-12.5	-17.1	-32.3	-1.1	M1	5.45	+0.23	+7.77	-0.45	
735	(8.52)	1.08	0.088	99/-57	-13.5	+9.7	-9.0	-6.9	M2	5.34	-0.10	+8.25	+0.62	X
740	7.47	0.765	0.091	-202/-1213	+10.6	-46.8	-40.4	-19.4	M2 V	5.05	+0.60	+7.27	+0.17	
752A	6.92	1.00	0.168	-572/-1346	+35.2	+53.3	-8.6	-5.6	M3.5 V	5.03	+0.31	+8.05	+0.46	X
752B	12.71	1.83							M8 V	--	--	+13.84	-1.55	X
775	6.45	0.41	0.071	-84/122	-31.3	+23.8	-16.5	+16.2	K4	5.98	+0.12	+5.71	+0.11	
793	8.24	1.075	0.124	455/275	+10.0	+20.1	+8.5	-5.7	M3	5.11	+0.4	+8.71	+0.14	
798	7.42	0.60	0.080	70/-1665	-43.7	+49.2	-52.6	+26.6	K7 V	4.97	+0.89	+6.94	-0.25	
809	6.79	0.81	0.140	6/-778	-18.7	-22.3	-11.8	-20.2	M2 V	5.09	+0.50	+7.52	+0.12	
820A	4.12	0.46	0.296	4139/3182	-64.7	+90.5	-53.7	-8.9	K5 V	5.75	+0.29	+6.48	-0.43	X
820B	4.67	0.60							K7 V	5.49	+0.37	+7.03	-0.39	X
821	8.96	0.855	0.093	713/-1971	-45.0	+8.7	-109.3	-3.4	M3	4.48	+1.06	+8.80	-0.95	
845	3.75	0.395	0.291	3990/-2558	-40.0	+77.4	-38.1	+4.0	K5 V	5.85	+0.27	+6.08	-0.33	
873	7.69	1.18	0.195	-701/-440	-2.1	-20.5	+1.4	-1.2	M4	5.49	-0.37	+9.14	+0.19	X
875	8.15	0.725	0.070	-120/120	-7.0	-1.6	+5.8	+11.5	M1	4.96	+0.74	+7.38	-0.12	
879	5.45	0.425	0.128	332/-165	+7.0	+5.7	+8.3	-11.6	K5 V	5.98	+0.11	+5.99	-0.10	X
887	5.51	0.835	0.279	6781/1305	+9.7	+10.20	-14.8	-56.8	M2 V	4.97	+0.59	+7.74	+0.02	
908	7.07	0.855	0.175	1001/-963	-71.7	+9.1	-72.4	+38.6	M2 V	4.88	+0.66	+8.09	-0.24	

Notes to TABLE 2.

2, 4AB ADS 48. No. 2 is 328 arcsec from 4AB. The components of No. 4 show orbital motion and are separated by about 10 arcsec.

15AB 40 arcsec separation.

82 Equal component binary.

105AB 165 arcsec separation. The B component has probably one of the least active, chromospheres known and is a close binary with a companion at (M_I, R-I) = (+13.13, +4.4:) mag (Golimowski et al. 1995).

109 UX Ari.

166AC 84 arcsec separation. B is a white dwarf companion to C.

195A ADS 3841H. 194 is alpha Aur, 721 arcsec distant.

277AB 39 arcsec separation. A is VV Lyn and an astrometric binary with P = 44y (Heintz 1993).

278C YY Gem, eclipsing binary with equal components and P = 0.81d. 72 arcsec from alpha Gem (278AB), a visual binary in which the bright component is also a Sp.B.

285 YZ CMi, very probably a pre-main sequence member of the Pleiades supercluster.

338AB ADS 7251, 19 arcsec separation.

360/2 89 arcsec separation. Pre-main sequence?

412A B is WX UMa, 28 arcsec distant.

551 Proxima Cen.

570AB ADS 9446, 20 arcsec separation. B is a Sp.B. and interferometric double with the components differing by about 1.6 mag.

617AB 63 arcsec separation. B is probably a close binary.

653/4 187 arcsec separation.

669AB 16 arcsec separation. V 647 and V 639 Her.

720AB B is VB 9, 112 arcsec distant.

725AB ADS 11632, 14 arcsec separation. P = 408 y, a = 13.88 arcsec (Heintz 1987).

729 V 1216 Sgr.

735 V 1285 Aql. Sp.B. P = 10.3d. Probable rapid variation of CaII flux.

752AB B is VB 10, 74 arcsec distant and possible brown dwarf. A may be undetected binary.

820AB 61 Cyg.

873 EV Lac.

879 Cpm with alpha PsA, 2 degrees distant.

The available astrometric data for all of these stars is quite uncertain and the proper motions are mainly from parallax solutions. The trigonometric parallax of Gliese 181.1 depend on a single Yale determination, that for G48−25 is from a single Sproul result, and G10−25 may be an astrometric binary with a period of 540 days and parallaxes of 0.023(V) arcsec to 0.056(D) arcsec have been determined. The results for these objects are represented in Fig. 4 with clear circles.

D. The only known member of the Kapteyn's star group in the relevant temperature range is Kapteyn's star (Gliese 191) itself:

$$I = 7.06 \text{ mag}, \qquad M_I = +9.06 \text{ mag},$$
$$R-I = 0.80 \text{ mag}, \qquad \Delta M_I = -1.46 \text{ mag},$$
$$\pi(\text{Trig}) = 0.252 \text{ arcsec}.$$

This star is represented by a closed circle in Fig. 4.

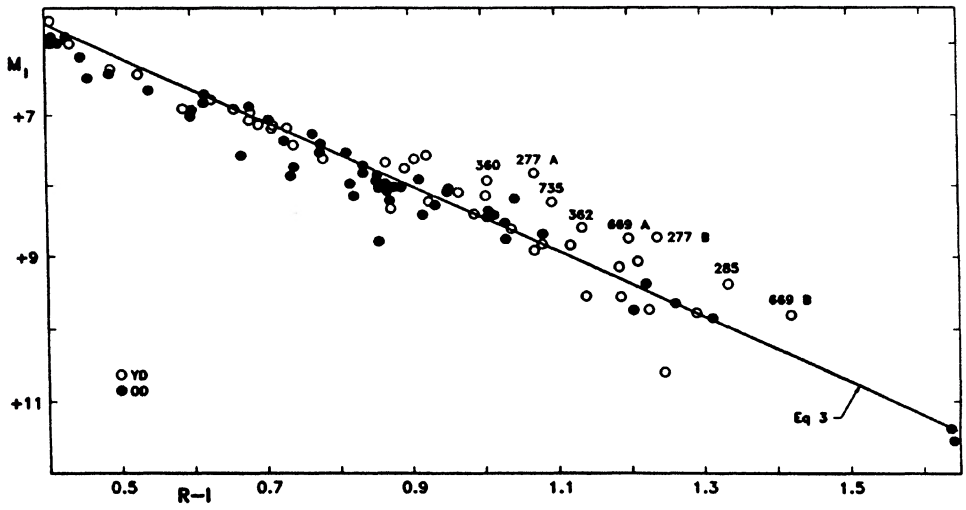

FIG. 2. The stars of Table 2 in the (M_I, $R-I$) plane.

E. Monet *et al.* (1992) have isolated 17 extreme subdwarfs with high accuracy parallaxes (*m.e.* ~0.001 arcsec). These stars, with the identifications given by Monet *et al.* and photometry derived from that published by them, are listed in Table 3 together with the parallaxes and the resulting space motion vectors, U, V, W. The stars for which radial velocity is not available have the percentage of the velocity, that contributes to U, V, and W, listed in parenthesis. Two additional stars, with larger parallaxes, have been added by Ruiz & Anguita (1993) and are at the end of Table 3. These extreme subdwarfs are indicated by crosses in Fig. 4. The luminosities of these stars can be tested with the faint companion, VB 12, to the *F*-type subdwarf binary ADS 16644AB, which is HD 219617(G273−1), a high proper motion (1.3 arcsec/yr^{-1}) visual binary with a period of 104 yr and $a=0.402$ arcsec (Heintz 1991). Because of the equal components, the quadrant of the angular separation is uncertain, so a possible (but unlikely) solution gives a period of 280 yr and $a=0.800$ arcsec. This uncertainty leads to a very-little difference in the mass function, a^3/P^2. The orbit is otherwise well determined. A third component, VB 12 (van Biesbroeck 1961) is 15 arcsec distant and, from observations with the AAT,

	I	$R-I$
ADS 16644AB	($8^m.54$)	$0^m.205$,
VB 12C	14.54	0.88.

The I magnitude of AB has been corrected for equal components. If the companion is similar to the extreme subdwarfs, represented by crosses in Fig. 4, $M_I \sim +10.6$ mag, giving a modulus of 3.95 mag and $\pi=0.016$ arcsec, or a mean mass of the bright component of 0.75 solar masses for the short period and 0.8 solar masses for the long period. The mean component then lies near the knee of the evolved main sequence in a metal weak globular cluster. Trigonometric parallax determinations range from 0.002 arcsec by the Cape observers to 0.040 arcsec from the Yale observations. The mass derived here is the same as that predicted by models for metal poor globular cluster members at the knee of the evolved main sequence (e.g., VandenBerg & Bell 1985). In summary,

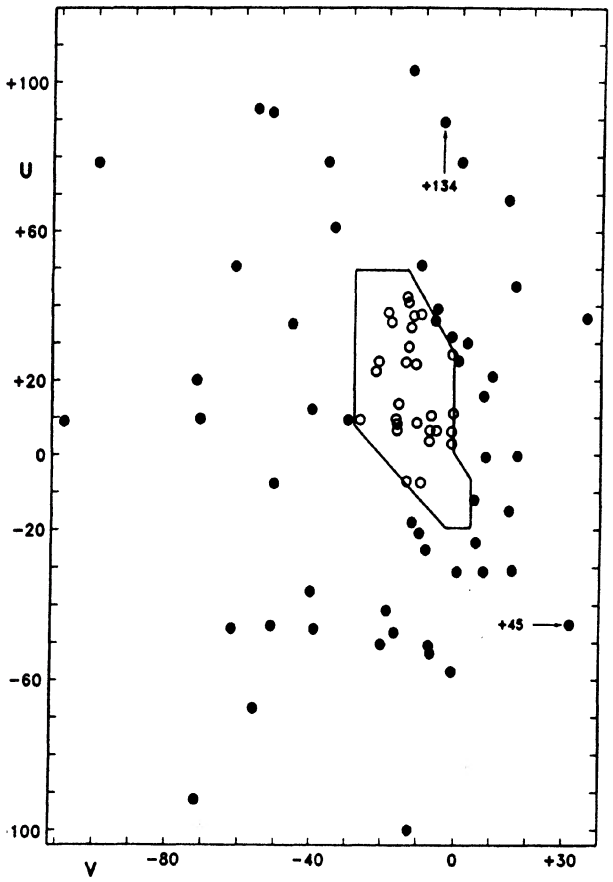

FIG. 3. The stars of Table 2 in the (U,V) velocity plane. U is positive in the direction away from the galactic center and V is positive in the direction of galactic rotation.

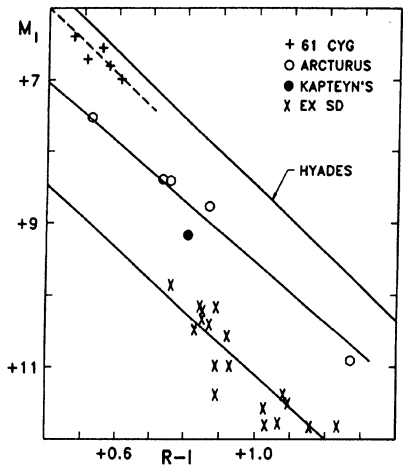

FIG. 4. The main sequence displacement for stars of various abundances.

	ΔM_I	[Fe/H]
Hyades	0.00	0.1
61 Cyg	−0.29	0.0 to −0.1
Arcturus	−1.16	−0.5 to −0.7
Kapteyn's	−1.46	−1.0 to −1.5
Extreme sd	−2.7	−2.5: to −3.5.

The photometric values of P[Fe/H], as well as the spectroscopic determinations of [Fe/H] range from 0.0 to −0.1 dex for the components of 61 Cyg. Recent spectroscopic results for Arcturus give [Fe/H] between −0.5 and −0.7 dex and this range is reflected in the photometric results for group dwarfs. The photometric estimates of the heavy element abundance for main sequence members of Kapteyn's star

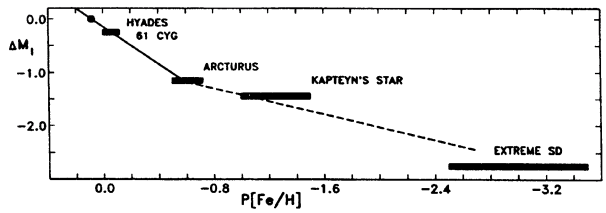

FIG. 5. The main sequence displacement as a function of heavy element abundance.

group range from [M/H]=−1.0 to −1.7. A single spectroscopic determination (Mould 1976) gives [Ti/H]=−0.5±0.3 dex and [Ca/H]=−1.2±0.5 dex for the eponymous star. No reliable results are available for the extreme subdwarfs but an extensive spectroscopic analyses of HD 219617, the bright companion to VB 12, should be possible. Several early results (Cayrel de Strobel *et al.* 1985) indicated values of [Fe/H] near-1.4 dex. From the known total range of metallicities the values of −2.5 to −3.5 for extreme subdwarfs are guesses only. The correlation shown in Fig. 5 suggests that the rate of increases in ΔM_I slows markedly for values of [Fe/H] less than about −1 dex.

If the (T_e, $R-I$) relation is independent of abundance, Fig. 4 reflects the dependence of the (M_{BOL}, log T_e) relation on chemical composition. However, several models (e.g., F. Allard, as quoted by Monet *et al.* 1992) suggest a strong dependence of the (T_e, $R-I$) relation on [Fe/H] for the coolest stars ($R-I>0.7$ mag) and when this is allowed for, the luminosity-temperature array shows very little dependence on [Fe/H]. This is contrary to the model results of VandenBerg *et al.* (1983) which, at log T_e=3.60 ($R-I$ =0.67 mag), M_{BOL}([Fe/H]=−2.3 dex)−M_{BOL}([Fe/H]

TABLE 3. Extreme subdwarfs.

LHS	π Trig	μ_α/μ_δ 0".001	ρ km/sec	M_I	R-I	U	V	W	ΔM_I
1174	0".0157	368/-508	–	+11.0	0.88	+34(+40)	-155/+57	-104(-72)	-3.0
192	0.0102	624/-862	–	+10.5	0.82	+65(+96)	-476(+16)	-39(-24)	-2.8
1742a	0.0134	373/-307	–	+11.8	1.22	-119(+97)	-247(-5)	+157(-20)	-2.3
205a	0.0104	404/-912	-117	+11.8	1.02	+177	-453	-36	-3.2
LP251-35	0.0167	476/+637	–	+0.45	0.86	+56(+98)	-450(+18)	-156(+2)	-2.6
1970	0.0129	279/-936	-7	+11.4	0.88	+190	-310	-54	-3.4
2045	0.0111	326/-387	–	+11.4	1.07	-154(+67)	-145(-58)	+41(+47)	-2.6
3061	0.0089	-391/-406	–	+11.8	1.15	-32(-56)	-293(+21)	+54(+80)	-2.6
3168	0.0058	-347/-360	–	+10.6	0.91	-28(-84)	-405(+12)	+48(+52)	-2.5
3178	0.0071	-485/-454	–	+11.0	0.92	-130(-61)	-429(+42)	+150(+67)	-2.9
3259	0.0064	-474/-194	–	+10.4	0.84	-2(-89)	-318(+25)	+205(+39)	-2.6
453	0.0103	-860/551	-1	+11.0	0.94	-230	-175	+353	-2.8
3382	0.0104	-22/861	-155	+10.2	0.84	-280	-243	-75	-2.4
3390	0.0123	-380/354	–	+11.5	1.08	+107(-17)	-52(+90)	+160(+41)	-2.6
3548	0.0083	-308/-772	+49	+10.2	0.88	+335	-348	-46	-2.2
3628	0.0088	-524/-441	–	+10.2	0.85	-270(-66)	-216(+47)	+130(-58)	-2.4
3868	0.0054	398/-368	–	+9.9	0.755	+131(-5)	-275(+79)	-366(-61)	-2.5
375	0.040	-1385/-34	+169	+11.6	1.015	-18	-181	+149	-3.0
407	0.032	-1230/-614	+211	+11.8	1.045	-122	-223	+144	-3.1
								mean	-2.7

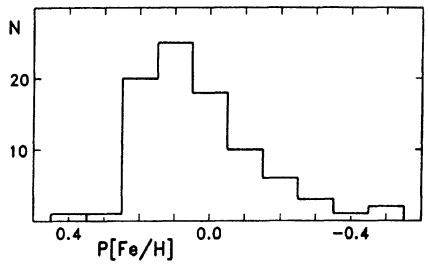

FIG. 6. The distribution of photometric abundances, (P[Fe/H]) for stars in Table 2.

$=-1.3$ dex)$\sim$1 mag and $M_{\rm BOL}$([Fe/H]=0 dex) $-M_{\rm BOL}$([Fe/H]-1.3 dex)$\sim$1.25 mag. These are very similar results to those seen in Fig. 4, indicating that there is little or no dependence of the (T_e, $R-I$) relation on heavy element abundance. In any event, over the range of ($R-I$) discussed here the parallel stratification of the (M_I, $R-I$) relation, as a function of [Fe/H], is obvious.

The stars in Table 2 all have $\Delta M_I > -0.1$ mag, or [Fe/H]$\geqslant -0.6$ dex and the linear relation, indicated by the solid line in Fig. 5,

$$[\mathrm{Fe/H}] = 0.625\Delta M_I + 0.125, \quad (4)$$

closely represents the observations. This leads to the distribution of [Fe/H] values shown in Fig. 6. The probable pre-main sequence stars discussed above are omitted from this figure. At the distance of the stars in Table 2 a 5% error in the parallax will lead to negligible error in [Fe/H]. It should be noted that if the nine stars identified here as pre-main-sequence objects are, instead, displaced from the main sequence because of large overabundances of heavy elements, the histogram in Fig. 6 would be curiously skewed with a total of ten stars having [Fe/H]$-+0.4$ to $+0.6$ dex.

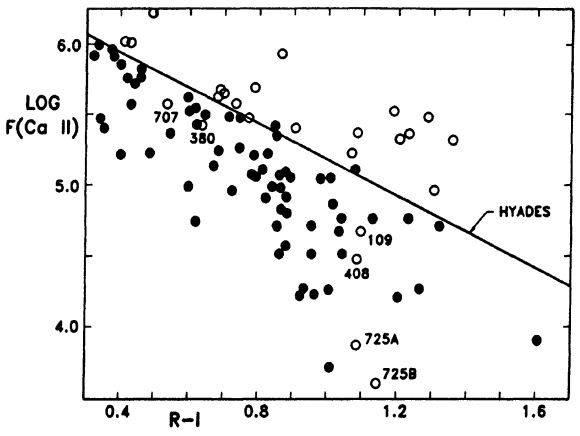

FIG. 7. The old disk (closed circles) and young disk (open circles) stars, judged by their position in the (U,V) plane (Fig. 3), in the log F(Ca II), $R-I$ plane. The Hyades supercluster members, which are amongst the oldest young disk stars, are represented by a straight line.

4. STELLAR SURFACE FLUXES OF Ca II AND AGE

The young and the old disk population stars have been found to occupy mutually exclusive domains in the (U,V) velocity plane (e.g., Eggen 1989a, 1995c). This separation is tested with the log F(Ca II) and ($R-I$) values listed in Table 2 and shown in Fig. 7. Open and closed circles in the figure represent, respectively, stars in the young disk and old disk domains of Fig. 3. The straight line in Fig. 7 represents the Hyades ($t\sim 10^9$ yr), interpolated between Eqs. (1) and (2);

$$\log F(10^9 \text{ yr}) = 6.46 - 1.28(R-I) \quad \text{Hyades.} \quad (5)$$

The Hyades stars are near the upper age limit of YD objects and, as seen in Fig. 7, Eq. (5) separates the two population with the exception of a half dozen, labeled YD stars;

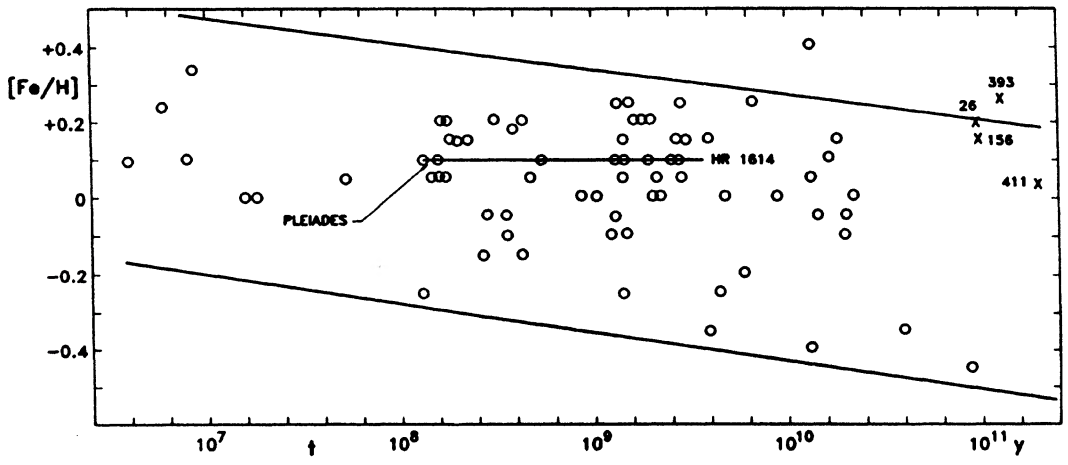

FIG. 8. The correlation between the heavy element abundances and the photometric ages. The range of ages covered by the Pleiades, Hyades and HR 1614 superclusters, all of the same metal abundance, is indicated by a straight line. The probably anomalous ages for Gliese 26, 156, 393, and 411 are discussed in the text.

Gliese	$R-I$	π Trig	U	V km/s	W	log F Ca II	Δ log F
109	1.055	0.133	+40.5	−15.9	−12.8	4.67	+0.58
380	0.62	0.222	+6.9	−19.1	−35.0	5.40	+0.44
408	1.035	0.145	+8.0	−12.6	−4.4	4.44	+0.87
707	0.53	0.073	+9.4	−18.7	−19.3	5.56	+0.39
725A	1.07					3.88	+1.38
		0.290	+24.2	−13.1	+24.9		
725B	1.135					3.63	+1.52.

Considering the uncertainties and the possible intrinsic variations in log F, the population separation is clear. However, if log F is truly indicating the stellar age, a small percentage of young disk stars, on the basis of their motion, have ages comparable with old disk objects. The most extreme case involves the components of Gliese 725, both of which appear to be amongst the oldest stars in Fig. 7. However, the values of log F are from an unpublished thesis (Mathioudakis 1992) and are at odds with the log F(Mg II) values taken, unfortunately, also from an unpublished thesis (Panagi & Mathioudakis 1993). Obviously new data are necessary before these results can be accepted. In any case, a further study of the Ca II flux from Gliese 109, 380, 408, and 707 is required. Also, the W velocity of 35 km/s for Gliese 380 is larger than any other YD star discussed here and may exceed the expected cap on values of YD stars. Additional log F data are necessary before the possibility that up to 10% of the YD stars, selected on the basis of the (U,V) velocity, may have ages greater than 10^9 yr can be accepted. Simon (1992, Fig. 3) has demonstrated with Mg II fluxes that the separation between populations, seen in Fig. 7, can be extended to the subdivision of ages within the young disk, although the small range of ages involved in that subdivision shows some overlap caused by the inherent instability of the individual fluxes.

The fact that the Pleiades and HR 1614 supercluster members all populate the same main sequence ([Fe/H]~0.1–0.2 dex) leads to a minimum range of about 10^8–4×10^9 yr for a given heavy element abundance. Equations (1) and (2) and the discussion in Eggen (1990) lead to $\Delta t^{1/3}\sim\Delta F$(Ca II), or

$$\log t = 2.87\ \Delta\ \log F(\text{Ca II}) + 8.00, \quad (6)$$

where Δ log F is listed in Table 2. The values of [Fe/H] from Eq. (4) and t from Eq. (6), for most of the stars in Table 2, are correlated in Fig. 8. The pre-main-sequence objects discussed in Sec. 3 and Gliese 735AB, discussed in the previous paragraph, are omitted. The four stars shown as labeled crosses in Fig. 8 have extreme values of t which may be suspect. For example, the value of log F(Ca II) for Gliese 26 and 156 are from an unpublished thesis (Mathioudakis 1992) and need to be confirmed as do the Ca II fluxes for Gliese 393 and 411.

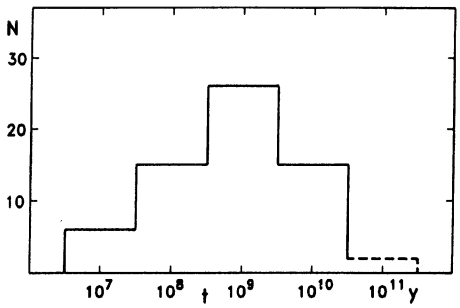

FIG. 9. The distribution of photometric ages for the stars in Table 2.

The distribution of stars in Fig. 8 indicates very little decrease in the age range for a given [Fe/H], with decreasing [Fe/H] amongst disk stars. The distribution of the derived ages for these stars is shown in Fig. 9.

5. SUMMARY

(1) A study of a sample of stars within 14 pc of the sun isolates nine probable pre-main sequence objects; Gliese 277A and B, 285, 360/2, 382, 669A and B, and 735.

(2) The remaining stars in the sample have a heavy element abundance range from [Fe/H]=+0.4 to −0.5 dex, based on main sequence displacement.

(3) The lower main sequence in the $(M_I, R-I)$ plane consists of parallel sequences with their zero point a function of [Fe/H]. These main sequences are linear between $R-I=0.4(T_e=4650$ K) mag and $1.2(T_e=3220$ K) mag; this linearity continues, for the Hyades stars, to $R-I=1.6(T_e=2900$ K), near the end of the hydrogen burning main sequence.

(4) The possibility that as many as 10% of the stars falling in the young disk domain of the (U,V) velocity plane are older than about 2×10^9 yr needs a more consistent data set of Ca II flux observations of a larger sample of parallax stars.

(5) An accurate determination of the rate of change of the zero point of the main sequence as a function of the change in heavy element abundance for [Fe/H]<−0.6 dex needs extensive abundance determinations for extreme subdwarfs.

(6) The correlation of [Fe/H] with age for lower main sequence stars near the sun shows a very slow decrease in both the mean abundance and the abundance range with increasing age.

REFERENCES

Andrews, A. D., and Staneck, K. Z. 1993, A&A, 279, 197
Burrows, A., Hubbard, W., Saumon, D., & Lunine, J. 1993, ApJ, 406, 158
Carlsberg Meridian Catalogues 1991, Copenhagen University Obs.
Cayrel de Strobel, G., Bentolila, C., Hauck, B., & Duquennoy, A. 1985, A&AS, 59, 145
Duquennoy, A., & Mayor, M. 1988, A&A, 200, 135
Eggen, O. J. 1982, ApJS, 50, 221
Eggen, O. J. 1983, AJ, 88, 813
Eggen, O. J. 1989a, PASP, 101, 366
Eggen, O. J. 1989b, Fund Cosmic Phys., 13, 1
Eggen, O. J. 1990, PASP, 102, 166
Eggen, O. J. 1992, AJ, 104, 1906
Eggen, O. J. 1993, AJ, 106, 1885
Eggen, O. J. 1995a, AJ (in press)
Eggen, O. J. 1995b, AJ (in press)
Eggen, O. J. 1995c, AJ (in press)

Geyer, D., Harrington, R., & Worley, C. 1988, AJ, 95, 1841
Gliese, W. 1969, Veroff Astron. Reichen-Inst., Heidelberg No. 22
Golimowski, D., Nakajima, T., Kulkarni, S., & Oppenheimer, B. 1995, ApJL (in press)
Harrington, R., *et al.* 1985, AJ, 90, 123
Heintz, W. 1987, PASP, 99, 1084
Heintz, W. 1989, A&A, 217, 145
Heintz, W. 1991, A&AS, 90, 314
Heintz, W. 1993, AJ, 105, 1188
Hufnagel, B., & Smith, G. 1994, PASP, 106, 1068
Leggett, S., Harris, H., & Dahn, C. 1994, AJ, 108, 944
Mathioudakis, M. 1992, Ph.D. thesis, Queen's University, Belfast
Monet, D., Dahn, C., Vrba, F., Harris, H., Pier, J., Luginbuhl, B., & Ables, H. 1992, AJ, 103, 638
Mould, J. 1976, ApJ, 210, 402
Mould, J. 1978, ApJ, 226, 923
Panagi, P., & Mathioudakis, M. 1993, A&AS, 100, 343
Prosser, C., Stauffer, J., & Kraft, R. 1991, AJ, 101, 1341
Ruiz, M. T., & Anguita, C. 1993, AJ, 105, 614
Russell, H. N. 1912, AJ, 27, 96
Simon, T. 1992, ASP Conf. No. 26, 3
Stauffer, J., & Hartmann, L. 1986, ApJS, 61, 531
Van Biesbroeck, G. 1961, AJ, 66, 424
VandenBerg, D. A., & Bell, R. A. 1985, ApJS, 58, 561
VandenBerg, D. A., Hartwick, F. D. A., Dawson, P., & Alexander, D. R. 1983, ApJ, 266, 747